

The Non-Planar Four-Point Integrand and Konishi Dimension in $\mathcal{N} = 4$ Super Yang–Mills Theory at Five Loops

Till Bargheer* and Albert Bekov†

Deutsches Elektronen-Synchrotron DESY, Notkestr. 85, 22607 Hamburg, Germany

We compute the complete non-planar integrand for the correlation function of four lightest scalar operators in $\mathcal{N} = 4$ super Yang–Mills theory at five-loop order. This is equivalent to the super-correlator of nine stress-tensor multiplets in the self-dual theory. Starting with an ansatz of f -graphs, we impose constraints from light-cone limits, and fix the remaining freedom by using the reformulation of the theory in twistor space. We develop an efficient GPU-based algorithm for the numerical evaluation of the twistor rules. As an application, we extract the five-loop non-planar anomalous dimension of the Konishi operator. Our code and result are provided in ancillary files.

I. INTRODUCTION

The correlator of four lightest ($\mathbf{20}'$) scalar BPS operators $\mathcal{O}(x, y) = \text{Tr}[(y \cdot \phi(x))^2]$ in $\mathcal{N} = 4$ SYM has been studied extensively at weak [1–12] as well as strong and finite coupling [13–27]. It is the simplest correlator with a non-trivial coupling dependence, contains information on many observables through OPE and cusp limits, and is related to phenomenologically interesting quantities such as event shapes and energy-energy correlators [28–30].

At weak coupling, the loop correlator can be computed by integrating over Lagrangian insertions [4, 31, 32],

$$G_4 = \langle \mathcal{O}(x_1, y_1) \mathcal{O}(x_2, y_2) \mathcal{O}(x_3, y_3) \mathcal{O}(x_4, y_4) \rangle = \sum_{\ell \geq 0} a^\ell \int \frac{d^4 x_5 \dots d^4 x_{4+\ell}}{(-1)^\ell \ell!} G_4^{(\ell)}(x_i, y_i), \quad (1)$$

$$G_4^{(\ell)}(x_i, y_i) = \langle \mathcal{O}_1, \dots, \mathcal{O}_4, \mathcal{L}_5, \dots, \mathcal{L}_{4+\ell} \rangle_0, \quad (2)$$

where $\mathcal{L}_i = \mathcal{L}(x_i)$ is the chiral interaction Lagrangian, $\langle \dots \rangle_0$ is the leading-order correlator, and $a = g_{\text{YM}}^2 N_c / (4\pi^2)$ is the 't Hooft coupling. Since \mathcal{O} and \mathcal{L} are components of the chiral stress-tensor multiplet,

$$\mathcal{O}(x, y, \theta) = \mathcal{O}(x, y) + \dots + (\theta)^4 \mathcal{L}(x), \quad (3)$$

the *integrand* $G_4^{(\ell)}$ inherits an $S_{4+\ell}$ permutation symmetry from the supercorrelator after factoring out a universal superinvariant, which allowed to bootstrap the planar integrand to twelve loops [6–12]. The non-planar integrand is known to four loops [7, 33]. Here, we push the computation of the non-planar integrand to five loops.

We explain our method in Section II, discuss the result in Section III, and extract the non-planar five-loop Konishi anomalous dimension in Section IV. Technical details are presented in appendices. Our code and result are available in ancillary files.

II. METHOD

We adopt the approach used in the four-loop computation [33], utilizing the twistor reformulation of the theory.

Due to its larger gauge freedom, this framework offers a simpler set of Feynman rules, at the cost of introducing a fixed reference twistor, which does not affect the final result, yet is practically impossible to eliminate. We therefore resort to using a manifestly invariant ansatz for the non-planar integrand, and fix its coefficients by numerically matching against the twistor answer. This is particularly efficient for the four-point integrand, where a compact ansatz in so-called f -graphs is available.

The main difficulty at five loops, beyond the overall large number of graphs, are the contractions of 20 Grassmann variables introduced in the twistor Feynman rules. These make the numerical evaluation very costly, such that it cannot be performed on an average computer. We solve this problem by implementing a fast GPU-based algorithm, which substantially accelerates the contraction process.

f -graph ansatz. The Born-level correlator of four stress-tensor operators and $\ell > 0$ chiral on-shell Lagrangians takes the form [7, 34]

$$G_4^{(\ell)}(x_i, y_i) = 2 \frac{N_c^2 - 1}{(4\pi^2)^{4+\ell}} R(x_i, y_i) \xi_4 F^{(4+\ell)}(x_i), \quad (4)$$

where $R(x_i, y_i)$ is the unique superconformal invariant of four points and $\xi_4 = x_{12}^2 x_{13}^2 x_{14}^2 x_{23}^2 x_{24}^2 x_{34}^2$. $F^{(n)}$ is a rational function of x_{ij}^2 that is invariant under all permutations of x_1, \dots, x_n , has at most simple poles in x_{ij}^2 , and conformal weight $+4$ in each point x_i . This function can be expanded in so-called f -graphs, $F^{(n)} = \sum_{i=1}^{N_n} c_i^{(n)} f_i^{(n)}$, where each $f_i^{(n)}$ represents a permutation-invariant sum of terms, normalized such that each term appears with unit coefficient. The total number of f -graphs N_n is listed in Table I. The color dependence of $G_4^{(\ell)}$ is encoded in the coefficients $c_i^{(n)}$, which are polynomials in $1/N_c^2$. Thus we can define the genus expansion of $F^{(n)}$ by

$$F^{(n)} = \sum_{g \geq 0} \frac{1}{N_c^{2g}} F^{(g,n)} = \sum_{g \geq 0} \frac{1}{N_c^{2g}} \sum_{i=1}^{N_n} c_i^{(g,n)} f_i^{(n)}, \quad (5)$$

where $c_i^{(g,n)}$ are now purely numerical coefficients.

It has been conjectured that the integrand $G_4^{(g,\ell \geq 2)}$ only depends on f -graphs up to genus g [7]:

$$c_i^{(g,n)} = 0 \quad \text{if} \quad \text{genus}(f_i^{(n)}) > g, \quad (6)$$

* till.bargheer@desy.de

† albert.bekov@desy.de

| n | \mathcal{N}_n | genus | | | Gram id. |
|-----|-----------------|-------|-----|----|----------|
| | | 0 | 1 | 2 | |
| 7 | 4 | 1 | 3 | – | 1 |
| 8 | 32 | 3 | 29 | – | 3 |
| 9 | 930 | 7 | 833 | 90 | 208 |

TABLE I. Numbers of f -graphs \mathcal{N}_n entering the three-, four-, and five-loop ansatz, their genus distribution, and the number of linearly independent Gram identities.

where the genus of an f -graphs is defined as the minimal genus of the simple, connected graph obtained by associating an edge to each squared distance in the denominator. For planar integrands ($g = 0$), this implies that only the planar f -graphs contribute, which has been verified up to twelve loops [12]. In practice, we find the genus by using the algorithm `multi_genus` of [35], see Table I for the statistics.

In general, not all f -graphs are linearly independent. Since they are functions of squared distances x_{ij}^2 , they satisfy conformal Gram identities. These emerge when considering the $(n \times n)$ Gram matrix with elements

$$\mathcal{G}_{ij} = X_i \cdot X_j = x_{ij}^2 \quad \text{for } i, j = 1, \dots, n, \quad (7)$$

where X_i are the six-dimensional null vectors on which the conformal symmetry $\text{SO}(2, 4)$ acts linearly. This matrix is of rank six, implying that all (7×7) -minors vanish. After dividing by appropriate monomials in x_{ij}^2 , such that each point is of conformal weight $+4$, and symmetrizing over all n points, these conditions generate the Gram identities between the f -graphs.

Determining the four-point integrand amounts to finding the numerical coefficients $c_k^{(g,n)}$ in the ansatz (5). The freedom in the ansatz can be greatly reduced by imposing null or coincidence limits. At the planar level, such limits in fact uniquely determine the integrand up to twelve loops [6–12]. For the subleading $1/N_c^2$ terms, this is no longer the case: Some free coefficients remain, which have to be fixed by a numerical match with the twistor computation.

In order to constrain $F^{(g \geq 1, 9)}$, we impose the light-cone constraint [7]: Setting neighboring external operators to null separation ($x_{12}^2, x_{23}^2, x_{34}^2, x_{41}^2 \rightarrow 0$), the tree-level normalized correlator takes the form

$$\frac{G_4}{G_4^{(0)}} = 1 + 2 \sum_{\ell \geq 1} \frac{a^\ell}{(-4\pi^2)^\ell} \int \left(\prod_{k=5}^{4+\ell} d^4 x_k \right) \mathcal{F}^{(4+\ell)}(x_i), \quad (8)$$

where $\mathcal{F}^{(n)} = \lim_{x_{i,i+1}^2 \rightarrow 0} x_{13}^2 x_{24}^2 \xi_4 F^{(n)} / \ell!$ is the null-square limit of the tree-level normalized sum of f -graphs. While $\mathcal{F}^{(n)}$ is finite, the integrals in (8) diverge: Starting from $\ell = 2$, the ℓ -loop contribution to the logarithm of (8) exhibits a $\log^\ell(x_{i,i+1}^2)$ divergence [36]. However, the integrals of individual f -graphs generally produce stronger divergences $\log^k(x_{i,i+1}^2)$, $k > \ell$. These divergences arise from integration regions where one of the internal operators approaches one of the light-like segments. To ensure the correct logarithmic divergence of the corre-

lator, we require the *light-cone constraints*:¹ In the limit $x_5 \rightarrow \alpha x_1 + (1 - \alpha)x_2$, the integrand of the logarithm of (8) must vanish order by order in α . For the non-planar five-loop integrand, these conditions are:²

$$\lim_{x_5 \rightarrow \alpha x_1 + (1-\alpha)x_2} x_{15}^2 x_{25}^2 (\mathcal{F}^{(1,9)} - 2\mathcal{F}^{(1,8)} \mathcal{F}^{(0,5)}) = 0, \quad (9)$$

$$\lim_{x_5 \rightarrow \alpha x_1 + (1-\alpha)x_2} x_{15}^2 x_{25}^2 \mathcal{F}^{(g \geq 2, 9)} = 0. \quad (10)$$

For the genus-one integrand, following (6), one can impose that the 90 genus-two f -graphs do not contribute to the final integrand. Then, imposing (9) fixes all but 155 coefficients of $F^{(1,9)}$, of which 134 parametrize Gram identities. Hence, only 21 coefficients are left to be determined by the twistor computation.³ Starting from genus two, all 930 f -graphs contribute, and (10) fixes all but 23 coefficients, accompanied by 208 Gram identities, at every order in the genus expansion.

Twistor computation. We briefly summarize the steps necessary to compute the integrand of the four-point correlator using the twistor formulation. More details can be found in Appendix B.

First, all relevant skeleton graphs are generated. At ℓ -loop order, they are specified as all connected $(4 + \ell)$ -point graphs with $4 + 2\ell$ edges and a valency of at least 2 at each vertex, and can for example be obtained with the open-source program SAGE [37] (see Table II).

Second, starting from each skeleton graph \mathbf{g} , all associated ribbon graphs $\gamma \in \Gamma_{\mathbf{g}}$ can be formed by permuting over the order of the edges around each vertex. Then, the twistor Feynman rules are applied to these ribbon graphs: Each graph is dressed with a factor $(g_{\text{YM}}^2)^{P-V} (4\pi^2)^{-P}$, with P and V denoting the number of edges (propagators) and vertices of the graph. Every edge connecting vertices i and j is dressed with a propagator $d_{ij} = y_{ij}^2 / x_{ij}^2$. Each vertex i connected to cyclically ordered vertices j_1, \dots, j_k produces an R -factor $R_{j_1 \dots j_k}^i$ and a color trace $\text{Tr}(T^{a_{ij_1}} \dots T^{a_{ij_k}})$, where T^a denote the $\text{SU}(N_c)$ generators in the fundamental representation. For each ribbon graph γ , the traces can be evaluated to a function in N_c by successively applying the fusion and fission rules

$$\text{Tr}(T^a B T^a C) = \text{Tr}(B) \text{Tr}(C) - \text{Tr}(BC) / N_c, \quad (11)$$

$$\text{Tr}(B T^a) \text{Tr}(C T^a) = \text{Tr}(BC) - \text{Tr}(B) \text{Tr}(C) / N_c. \quad (12)$$

This yields an overall factor of $(N_c^2 - 1)N_c^\ell$ multiplied by a polynomial $c_\gamma(1/N_c^2)$. Furthermore, the dependence of the R -factors on the ribbon structure can be canonicalized by pulling out factors $\langle ijk \rangle$ via (cf. (B15))

$$R_{j_{\tau(1)} \dots j_{\tau(k)}}^i = R_{j_1 \dots j_k}^i \frac{\langle i j_1 j_2 \rangle \dots \langle i j_k j_1 \rangle}{\langle i j_{\tau(1)} j_{\tau(2)} \rangle \dots \langle i j_{\tau(k)} j_{\tau(1)} \rangle}, \quad (13)$$

¹ For the planar integrand, given by an ansatz in terms of planar f -graphs, this constraint fixes all seven coefficients.

² There are no further terms in (9) because $\mathcal{F}^{(1,n)} = 0$ for $n < 8$.

³ We further tested the five-loop ansatz against the cusp-limit constraint of [11]. This constraint turns out to be less restrictive and is already fully captured by the light-cone constraints.

where τ is a permutation. Let us denote the product of these kinematic factors for each canonicalized ribbon graph by $s_\gamma(\langle ijk \rangle)$. In this way, a universal product of propagators and R -factors can be pulled out of the sum over all ribbon graphs $\Gamma_{\mathbf{g}}$ associated to the same skeleton graph \mathbf{g} , leaving a sum that entails the complete dependency on the color structure $c_\gamma(1/N_c^2)$, and includes some kinematic factors $s_\gamma(\langle ijk \rangle)$. Splitting the R -factors into basic factors R_{jkl}^i of Grassmann degree two (cf. (B13)), the sum of ribbon graphs over $\Gamma_{\mathbf{g}}$ can be schematically written as

$$\sum_{\gamma \in \Gamma_{\mathbf{g}}} \gamma = a^\ell \frac{N_c^2 - 1}{(4\pi^2)^{4+\ell}} p_{\mathbf{g}}(1/N_c^2, \langle ijk \rangle) \prod_{\mathbf{g}}^{4+2\ell} d_{ij} \times \prod_{\mathbf{g}}^{2\ell} R_{jkl}^i$$

with $p_{\mathbf{g}}(1/N_c^2, \langle ijk \rangle) = \sum_{\gamma \in \Gamma_{\mathbf{g}}} c_\gamma(1/N_c^2) s_\gamma(\langle ijk \rangle)$. (14)

Here, the symbol \mathbf{g} below the product signs indicate that the products only depend on the skeleton graph, not on the specific ribbon graph, while the number above denotes the number of factors in each product. The prefactors $p_{\mathbf{g}}$ encode the genus expansion, and can be evaluated for each skeleton graph at this stage. It is known that the full integrand is completely planar up to three loops, and there is a single correction of order $\mathcal{O}(1/N_c^2)$ at four loops. We find that the same is true at five loops: The prefactors $p_{\mathbf{g}}$ exhibit at most a $\mathcal{O}(1/N_c^2)$ contribution. This implies that $F^{(g \geq 2, 9)}$ vanishes, leaving only the remaining 21 coefficients of $F^{(1, 9)}$ to be determined.

Third and finally, each skeleton graph must be permuted over all inequivalent vertex labelings. This yields a large number of graphs \mathfrak{G} , in terms of which the integrand (4) can now be schematically expressed as

$$G_4^{(\ell)} = \frac{N_c^2 - 1}{(4\pi^2)^{4+\ell}} \sum_{\mathbf{g} \in \mathfrak{G}} \left(p_{\mathbf{g}} \prod_{\mathbf{g}}^{4+2\ell} d_{ij} \times \prod_{\mathbf{g}}^{2\ell} R_{jkl}^i \right). \quad (15)$$

To reduce the computational time of evaluating the expression, we aim to reduce the number of permuted graphs \mathfrak{G} to consider. As in [33], we choose a polarization in which all y_{ij}^2 vanish except y_{12}^2 and y_{34}^2 , which drastically cuts down the number of contributing graphs. Yet, the complete integrand is still accessible, since the polarizations only appear in the four-point invariant $R(x_i, y_i)$ in (4). Moreover, we can eliminate graphs that cannot generate the desired Grassmann monomial $\theta_5^4 \dots \theta_{4+\ell}^4$. For example, R -factors only depending on the external operators can be set to zero, and products of R -factors in which any internal label appears fewer than twice can also be removed. Listing the permutations, specifying the polarization, and removing non-contributing products of R -factors, we arrive at the second row of Table II. Some remaining graphs still evaluate to zero, despite it not being apparent from their symbolic expression. We remove such graphs by probing all remaining products of R -factors numerically, and keeping only graphs that are indeed non-vanishing. Their counts appear in the third row of Table II.

Let us mention that in four dimensions, the integrand $G_4^{(\ell)}$ has a pseudo-scalar contribution, which is produced

| ℓ | 1 | 2 | 3 | 4 | 5 |
|-------------------|---|----|-------|---------|-------------|
| # skeleton graphs | 3 | 11 | 63 | 513 | 5,553 |
| # permuted graphs | 1 | 73 | 6,321 | 732,288 | 110,732,441 |
| # non-zero graphs | 1 | 73 | 5,901 | 627,148 | 87,757,390 |

TABLE II. First row: Number of skeleton graphs generated with SAGE. Second row: Number of permuted and polarized graphs, excluding graphs that cannot produce the correct Grassmann monomial. Third row: Final number of graphs that have a non-vanishing contributions to the twistor result.

by a total derivative term in the twistor-reformulated action of $\mathcal{N} = 4$, and therefore vanishes upon integration. In Lorentzian signature, this contribution is imaginary, and hence can be numerically isolated. However, we perform the calculation in split signature, where the twistor computation remains real, such that we can efficiently employ finite fields. In order to isolate the pseudo-scalar contribution, we compute each numerical point twice, with kinematics that differ by a parity transformation. Taking their mean removes any pseudo-scalar contribution.

Grassmann contraction. One of the main challenges in evaluating the twistor expression numerically lies in the contraction of the Grassmann numbers that appear in the R -factors. Each term in the five-loop twistor expression (15) contains ten R -factors $\{R_1, \dots, R_{10}\}$, each quadratic in the Grassmann variables $\theta^{a\alpha}$, that must be contracted into the unique product $\theta_5^4 \dots \theta_9^4$ involving all 20 Grassmann numbers. Splitting each R_a into a list of the $\binom{20}{2} = 190$ products of Grassmann numbers, we find that the most efficient implementation iteratively contracts the R -factors into successively higher-degree products of Grassmann numbers as follows:

$$(S_a)^k = (t_{a-1})_{ij}^k (S_{a-1})^i (R_a)^j \quad \text{with } a \in [2, 10], \quad (16)$$

with $S_1 = R_1$, and t_a being fixed numerical sparse tensors that contract the vectors at each intermediate step. These successive tensor-vector-vector multiplications can be implemented highly efficiently on a graphics processing unit (GPU). Details on the tensors t_a and the GPU-based implementation of this algorithm are provided in Appendix C. Under optimal settings, the Grassmann contractions required to evaluate (15) at a single numerical point take approximately 17 hours on a single *Nvidia A100* GPU, rendering the determination of the 21 coefficients (each requiring the evaluation at two numerical points) in the five-loop genus-one ansatz practically feasible.

III. RESULT

As discussed above, the full five-loop integrand only consist of the planar part and the genus-one correction. By numerically matching against the twistor result, we can fix the remaining 21 free parameters in the genus-one ansatz, and find the full five-loop integrand. Of the 930 nine-point f -graphs, we excluded the 90 genus-two

graphs, as they do not contribute to the genus-one integrand. By adding an appropriate combination of the 134 Gram identities among the remaining graphs, we obtain a particular solution for the remaining 840 f -graph coefficients that exhibits the following properties: First, 582 coefficients are zero, thus the corresponding f -graphs do not contribute to the genus-one integrand. Second, the remaining 258 non-zero coefficients are of small integer value, as is visualized in Figure 4 in Appendix C. We provide this solution in the ancillary file `solution.m`.

Furthermore, we notice that a stronger statement than (6) might hold, namely the following: *The integrand $G_4^{(g, \ell \geq 2)}$ only depends on f -graphs of exactly genus g , that is*

$$c_i^{(g, n)} = 0 \quad \text{if} \quad \text{genus}(f_i^{(n)}) \neq g. \quad (17)$$

First, this is consistent with the non-planar integrands found so far. The genus-one correction to the four-loop integrand [7, 33] can be uniquely written in terms of the 29 genus-one eight-point f -graphs, using the three Gram identities to remove the dependency on the planar graphs. At five loops, we can construct a result in terms of only the genus-one f -graphs, reducing the Gram freedom to 127. Second, it immediately rules out $g \geq 2$ and $g \geq 3$ correction to the four- and five-loop integrand, respectively. Regarding the genus-two correction to the five-loop integrand, this statement implies that it is given in terms of the 90 genus-two nine-point f -graphs. Imposing the light-cone constraint (10) on this ansatz sets all but one coefficient to zero. The remaining f -graph vanishes in this limit, and thus trivially satisfies the constraint.⁴

IV. KONISHI ANOMALOUS DIMENSION

One of the immediate observables obtainable from the four-point $2\mathbf{o}'$ integrand is the anomalous dimension $\gamma_{\mathcal{K}}(a)$ of the Konishi operator $\mathcal{K}(x) = \text{Tr}(\phi(x) \cdot \phi(x))$, which is encoded in its two-point function. The latter can be extracted from the four-point correlator via the operator product expansion (OPE). \mathcal{K} dominates the OPE, thus $\gamma_{\mathcal{K}}(a)$ can be extracted by double-pinching the integrand ($x_2 \rightarrow x_1$ and $x_4 \rightarrow x_3$) [38]:

$$\begin{aligned} \log \left(1 + 6 \sum_{\ell \geq 1} \frac{a^\ell}{(-4\pi^2)^\ell} \int \left(\prod_{k=5}^{4+\ell} d^4 x_k \right) \hat{F}^{(4+\ell)}(x_i) \right) \\ = \frac{1}{2} \gamma_{\mathcal{K}}(a) \log(u) + \mathcal{O}(u^0), \end{aligned} \quad (18)$$

with $u = x_{12}^2 x_{34}^2 / (x_{13}^2 x_{24}^2)$ being one of the conformal cross-ratios and

$$\hat{F}^{(n)} = \lim_{\substack{x_2 \rightarrow x_1 \\ x_4 \rightarrow x_3}} x_{13}^4 \xi_4 F^{(n)} / \ell!. \quad (19)$$

Expanding the above equation to the genus-one five-loop order yields

$$\int \left(\prod_{k=5}^9 d^4 x_k \right) I^{(1,5)} = \frac{1}{2} \gamma_{\mathcal{K}}^{(1,5)} \log(u) + \mathcal{O}(u^0), \quad (20)$$

with $\gamma_{\mathcal{K}}^{(1,5)}$ denoting the genus-one five-loop correction to the Konishi anomalous dimension, and the integrand given by $I^{(1,5)} = -6(\hat{F}^{(1,5)} - 6\hat{F}^{(0,1)}\hat{F}^{(1,4)})/(4\pi^2)^5$. The log-divergence of the above integral arises when all of the integration points approach one of the external points x_1 or x_3 . In order to extract the coefficient $\gamma_{\mathcal{K}}^{(1,5)}$ in front of this divergence, we follow the steps outlined in [38]: First, we take $x_3 \rightarrow \infty$, effectively replacing all $x_{3k}^2 \rightarrow x_{13}^2$, to single out the divergence that arises when all points approach x_1 , and define $\hat{I}^{(1,5)} = \lim_{x_3 \rightarrow \infty} I^{(1,5)}$. Second, we apply dimensional regularization with $d = 4 - 2\epsilon$ and perform all but one integration

$$2 \int \left(\prod_{k=6}^9 d^{4-2\epsilon} x_k \right) \hat{I}^{(1,5)} = \frac{C^{(1,5)}}{\pi^2} (x_{15}^2)^{-2-4\epsilon}, \quad (21)$$

where $C^{(1,5)}$ is finite for $\epsilon \rightarrow 0$. The factor 2 is included to take into account the contribution of the integration around x_3 . Third, comparing with (18), a careful analysis on the infrared rearrangement of the remaining integration allows to identify the log-divergence by

$$-2 \int \frac{d^{4-2\epsilon} x_5}{\pi^2} (x_{15}^2)^{-2-4\epsilon} = \log u + \mathcal{O}(u^0) + \mathcal{O}(\epsilon), \quad (22)$$

in the leading behavior in ϵ . We refer for details on this regularization scheme to App. A in [38]. Finally, we identify $\gamma_{\mathcal{K}}^{(1,5)} = -C^{(1,5)}$, obtaining the correction to the anomalous dimension.

Practically, obtaining the genus-one five-loop anomalous dimension boils down to performing the four-loop propagator-type integration in (21). Starting from the obtained genus-one five-loop integrand $G_4^{(1,5)}$ and the known result of $G_4^{(1,4)}$ [7, 33], we construct $\hat{I}^{(1,5)}$ and find that $C^{(1,5)}$ is a linear combination of 2855 two-point four-loop integrals. Applying the integration-by-parts method, we reduce this linear combination of integrals to a small set of master integrals using the program FIRE6 [39, 40]. In particular, we find that it consists of 24 master integrals, 20 of which are associated to planar graphs, while the remaining integrals are associated to non-planar ones:

$$\gamma_{\mathcal{K}}^{(1,5)} = \left[\sum_{k=1}^{20} v_k \mathcal{J}_k + \sum_{k=1}^4 w_k \mathcal{I}_k \right]_{\epsilon \rightarrow 0}. \quad (23)$$

The coefficient functions v_k and w_k are expressed as expansions in ϵ . In particular, the leading order of each w_k is -1 . By introducing dual momenta, the master integrals corresponding to planar graphs can be transformed to four-loop propagator-type integrals in momentum representation. Graphically, these momentum master integrals are represented by the dual graphs of the original planar ones. The latter were explicitly calculated as expansions in ϵ in [41, 42], carried out to sufficiently high

⁴ An explicit expression for this f -graph is provided in line 843 of the ancillary file `allFGraphs.txt`. This behavior was already observed for the “8-point version” of this f -graph (cf. (5.25) in [7]).

orders, such that (23) can be evaluated at $\mathcal{O}(\epsilon^0)$. Of the four remaining master integrals associated to non-planar graphs, \mathcal{I}_1 and \mathcal{I}_2 were derived in [38] (cf. App. B therein). These integrals already appeared in the computation of the planar five-loop correction to the Konishi anomalous dimension. The explicit form and derivation of the final two master integrals \mathcal{I}_3 and \mathcal{I}_4 can be found in Appendix D.

Gathering the results of all master integrals and plugging them into (23), finally yields the non-planar contribution to the anomalous dimension of the Konishi operator at five loops:

$$\gamma_{\mathcal{K}}^{(1,5)} = 135\zeta_5 - \frac{234}{4}\zeta_3^2 + \frac{11907}{32}\zeta_7 \approx 430.657. \quad (24)$$

Importantly, all poles in ϵ vanish in the final result of the anomalous dimension, which is a strong consistency check of the derivation. Furthermore, $\gamma_{\mathcal{K}}^{(1,5)}$ does not depend on even Zeta values, which agrees with general expectations [43, 44] as well as existing data [45, 46]. More subtly, there are also no terms with transcendental weight zero and three. This is also the case for the non-planar correction of the four-loop Konishi anomalous dimension [46].

V. CONCLUSION

We have computed the full non-planar five-loop integrand of the correlator of four $\mathbf{20}'$ operators. The non-planar part is proportional to $1/N_c^2$, and it can be written exclusively in terms of genus-one f -graphs, with small integer coefficients. There are no genus-two contributions at five loops, which is consistent with all existing data. We also extracted the non-planar Konishi anomalous dimension (24), which consists of ζ_5 , ζ_3^2 , and ζ_7 terms. The dependence on N_c signifies that the radius of convergence

of the perturbative series shrinks at finite N_c as expected, see Appendix A.

We obtained the integrand from a combination of physical (light-cone) constraints, and input from a numerical twistor computation. An open question is whether the non-planar integrand could instead be fully determined by analytic constraints alone. For example, the non-planar part of the logarithm of G_4/G_0 may have at most $\log^{\ell-1}$ singularities at ℓ loops in the light-cone limit [7], which is not necessarily fully imposed by (9), (10). Further constraints could be derived by matching the f -graph periods [47] against the known completely integrated correlator [48, 49].

Our result encodes a wealth of five-loop non-planar OPE data, including the Konishi OPE coefficient [50], the twist-two spin- J anomalous dimensions and OPE coefficients [33, 38, 46], and the cusp anomalous dimension [51]. Extracting some of this data would provide valuable insight, particularly also because of their relevance to the respective QCD counterparts.

Acknowledgments. We are grateful to Gregory Korchemsky for illuminating correspondence, and to Sven Moch for comments on the manuscript. This work was funded by the Deutsche Forschungsgemeinschaft (DFG, German Research Foundation) Grant No. 460391856. We acknowledge support from DESY (Hamburg, Germany), a member of the Helmholtz Association HGF, and by the Deutsche Forschungsgemeinschaft (DFG, German Research Foundation) under Germany's Excellence Strategy – EXC 2121 “Quantum Universe” – 390833306. A.B. is further supported by the Studienstiftung des Deutschen Volkes. This research was supported through the Maxwell computational resources operated at Deutsches Elektronen-Synchrotron DESY, Hamburg, Germany.

Appendix A: The Konishi Dimension

For reference, we record the complete five-loop scaling dimension of the Konishi operator [46]:

$$\begin{aligned} \Delta_{\mathcal{K}} &= 2 + 3a - 3a^2 + \frac{21}{4}a^3 + \left(-\frac{39}{4} + \frac{9}{4}\zeta_3 - \frac{45}{8}\left[1 + \frac{12}{N_c^2}\right]\zeta_5\right)a^4 \\ &\quad + \left(\frac{237}{16} + \frac{37}{4}\zeta_3 - \frac{135}{16}\left[1 - \frac{16}{N_c^2}\right]\zeta_5 - \frac{9}{16}\left[9 + \frac{104}{N_c^2}\right]\zeta_3^2 + \frac{189}{12}\left[5 + \frac{63}{N_c^2}\right]\zeta_7\right)a^5 + \mathcal{O}(a^6) \\ &\approx 2 + 3a - 3a^2 + 5.25a^3 - \left(12.878 + \frac{69.993}{N_c^2}\right)a^4 + \left(36.64 + \frac{430.657}{N_c^2}\right)a^5 + \mathcal{O}(a^6). \end{aligned} \quad (A1)$$

The planar parts were found in [52], [4, 5], [53], [54–56], and [57–59] at one, two, three, four, and five loops, respectively. The four-loop $1/N_c^2$ non-planar correction term was found in [46]. The planar parts were re-derived in [38], which also established the method employed in this paper.

It is known that the weak-coupling expansion of the planar theory in the $N_c \rightarrow \infty$ limit converges for $a < 1/4$ [60]. The coefficients in the Konishi dimension (A1) indicate that the radius of convergence will shrink at finite N_c , as expected in a general Yang–Mills theory. A plot of the Konishi dimension for different values of N_c is

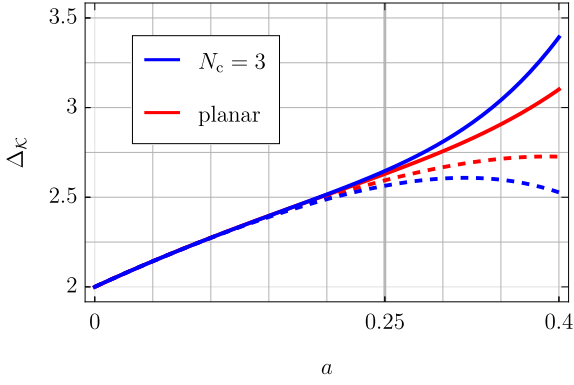


FIG. 1. The Konishi Dimension Δ_K as a function of the coupling a for $N_c = \infty$ (red) and $N_c = 3$ (blue) at four loops (dashed) and five loops (solid). The radius of convergence of the planar theory is at $a = 1/4$.

shown in Figure 1. Writing the Konishi dimension as

$$\Delta_K = 2 + \sum_{\ell=0}^{\infty} \gamma_K^{(\ell)} a^\ell, \quad (\text{A2})$$

we can estimate the radius of convergence as

$$\lim_{\ell \rightarrow \infty} \left| \frac{\gamma_K^{(\ell)}}{\gamma_K^{(\ell-1)}} \right| \approx \begin{cases} 1/0.25 & N_c = \infty, \\ 1/0.16 & N_c = 3, \end{cases} \quad (\text{A3})$$

see Figure 2. The number 0.25 for $N_c = \infty$ is expected, and the lower number 0.16 confirms that the radius of convergence shrinks at finite N_c .

Appendix B: Twistors

$\mathcal{N} = 4$ SYM theory can be formulated in the super-twistor space $\mathbb{CP}^{3|4}$, parameterized by homogeneous coordinates $\mathcal{Z} = (Z^I, \chi^A)$, consisting of complex three-dimensional projective coordinates Z^I and four Grassmann degrees of freedom χ^A . They are related to points in chiral Minkowski super-spacetime $(x^{\alpha\dot{\alpha}}, \Theta^{A\alpha})$ via the incidence relations

$$Z^I = (\lambda_\alpha, i x^{\dot{\alpha}\beta} \lambda_\beta) \quad \text{and} \quad \chi^A = \Theta^{A\beta} \lambda_\beta, \quad (\text{B1})$$

with λ_α being homogeneous coordinates. The fields in the theory are gathered in a superfield $\mathcal{A}(\mathcal{Z})$, that takes values in $(0, 1)$ -forms and belongs to the adjoint representation of $SU(N_c)$. The twistor action takes the form [61]

$$S(\mathcal{A}) = \int_{\mathbb{CP}^{3|4}} \mathcal{D}^{3|4} \mathcal{Z} \wedge \text{Tr} \left(\frac{1}{2} \mathcal{A} \bar{\partial} \mathcal{A} - \frac{1}{3} \mathcal{A}^3 \right) + \int d^4 x d^8 \Theta L_{\text{int}}(x, \Theta), \quad (\text{B2})$$

where $\mathcal{D}^{3|4} \mathcal{Z}$ is the canonical holomorphic volume on $\mathbb{CP}^{3|4}$. The first term is the self-dual part of the theory, whereas the second term describes the non-local interaction part

$$L_{\text{int}}(x, \Theta) = g_{\text{YM}}^2 (\log \det(\bar{\partial} - \mathcal{A}) - \log \det \bar{\partial}). \quad (\text{B3})$$

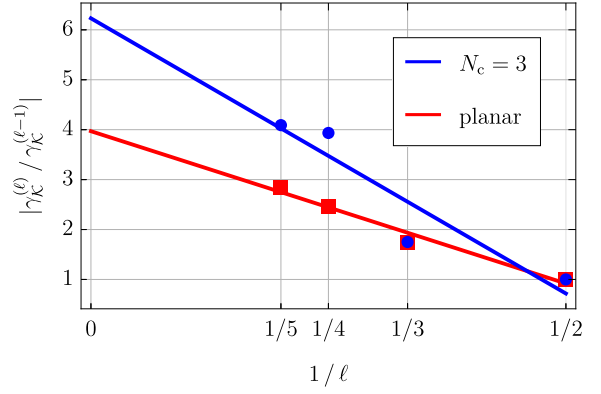


FIG. 2. Estimate of the convergence radius of the Konishi dimension weak-coupling expansion, for $N_c = \infty$ (squares, red) and for $N_c = 3$ (circles, blue). Shown are the ratios $|\gamma_K^{(\ell)}/\gamma_K^{(\ell-1)}|$ as in (A3), as a function of $1/\ell$, as well as linear fits whose intersections with $1/\ell = 0$ yield the numbers in (A3).

At this point, we can introduce the axial gauge, in which the cubic term of the self-dual part of the action vanishes, simplifying the following perturbative Feynman computations. In return, a fixed choice of a reference twistor Z_\star is introduced. While physical observables remain independent of this choice, all intermediate expressions will generally depend on it. Then, the propagator is defined by the remaining quadratic term

$$\langle \mathcal{A}^a(Z_1) \mathcal{A}^b(Z_2) \rangle = \bar{\delta}^{2|4}(Z_1, Z_2, Z_\star) \delta^{ab}, \quad (\text{B4})$$

where a, b denote the color indices of the fields, and $\bar{\delta}$ is a projective delta function. In order to describe the chiral, half-BPS stress-tensor multiplet $\mathcal{O}(x, y, \theta)$, we decompose the chiral superspace into two parts

$$\Theta^{A\alpha} = W_a^A \theta^{a\alpha} + Y_{a'}^A \psi^{a'\alpha}, \quad (\text{B5})$$

with the half-BPS condition implying the independence of the stress-tensor multiplet from $\psi^{a'\alpha}$. In supertwistor space, it is thus characterized by a subspace $\mathbb{CP}^{1|2}$, that can be parameterized by (λ, ψ) in the following way

$$Z(\lambda) = \lambda^1 Z_1 + \lambda^2 Z_2 = \lambda^\beta Z_\beta, \quad (\text{B6})$$

$$\eta(\lambda, \psi) = \lambda^\alpha \theta_\alpha^a W_a + \psi^{a'} Y_{a'}, \quad (\text{B7})$$

with $\psi^{a'} = \Psi^{a'\alpha} \lambda_\alpha$ and two choices of Z_β that define the twistor line corresponding to the point x . The stress-tensor multiplet can be expressed in twistor space as [62]

$$\mathcal{O}(x, y, \theta) = \int d^4 \Psi L_{\text{int}}(x, \Theta). \quad (\text{B8})$$

With these ingredients at hand, we can formulate the four-point loop-integrand $G_4^{(\ell)}$ as follows:

$$G_4^{(\ell)} = \int d^4 \theta_5 \dots d^4 \theta_{4+\ell} \langle \mathcal{O}_1 \dots \mathcal{O}_{4+\ell} \rangle_{\text{tree}} \Big|_{\theta_1, \dots, \theta_4 \rightarrow 0}, \quad (\text{B9})$$

where the expectation value is evaluated with respect to the twistor action (B2) at tree level, effectively setting

$L_{\text{int}} = 0$. Moreover, we abbreviate $\mathcal{O}(x_i, y_i, \theta_i) = \mathcal{O}_i$. Applying the axial gauge allows for a straightforward derivation of Feynman rules for the above correlation function. The connection between these rules and the usual Minkowski spacetime coordinates and polarization vectors can be made explicit by adopting the following parametrization

$$\begin{aligned} (Z_{i,\beta})_{\alpha}^{\dot{\alpha}} &= (\epsilon_{\alpha\beta}, x_{i,\beta}^{\dot{\alpha}}), \\ W_{i,a}^B &= (\delta_a^b, 0), \\ Y_{i,a'}^B &= (y_{i,a'}^b, \delta_{a'}^{b'}). \end{aligned} \quad (\text{B10})$$

With this choice, the resulting 4×4 determinants (denoted by angle brackets) compute the basic Lorentz and R-charge invariants, with unit proportionality factors

$$\langle Z_{i,1} Z_{i,2} Z_{j,1} Z_{j,2} \rangle \equiv \det(x_i - x_j)^{\dot{\alpha}\beta} = x_{ij}^2, \quad (\text{B11})$$

$$\langle Y_{i,1} Y_{i,2} Y_{j,1} Y_{j,2} \rangle \equiv \det(y_i - y_j)^{ab'} = y_{ij}^2. \quad (\text{B12})$$

While the twistor Feynman rules and their application was discussed in the main text, here we elaborate further on the structure and explicit expression of the R -factors that dress the Feynman graph vertices. As explained, each operator i that is connected to more than two vertices $j_1 \dots, j_k$ is dressed by an R -factor $R_{j_1 \dots, j_k}^i$, that exhibits a cyclic symmetry in its lower indices. These factors can be split into R -factors of valency three by using

$$R_{j_1 j_2 \dots j_k}^i = R_{j_1 j_2 j_3}^i R_{j_1 j_3 j_4}^i \dots R_{j_1 j_k - 1 j_k}^i, \quad (\text{B13})$$

where each valency-three R -factor is given by

$$R_{jkl}^i = -\frac{\delta^{0|2} (\langle ijk \rangle \psi_{il} + \langle ikl \rangle \psi_{ij} + \langle ilj \rangle \psi_{ik})}{\langle ijk \rangle \langle ikl \rangle \langle ilj \rangle}. \quad (\text{B14})$$

Here, we defined $\langle ijk \rangle = \epsilon_{\alpha\beta} \lambda_{ij}^{\alpha} \lambda_{ik}^{\beta}$. The parameters λ_{ij} and ψ_{ij} satisfy the following on shell conditions

$$\begin{aligned} \lambda_{ij}^{\alpha} &= \epsilon^{\alpha\beta} \frac{\langle Z_{i,\beta} Z_{j,1} Z_{j,2} \rangle}{\langle Z_{i,1} Z_{i,2} Z_{j,1} Z_{j,2} \rangle}, \\ \psi_{ij}^{a'} &= \epsilon^{a'b'} \frac{\langle Y_{i,b'} E_{ij} Y_{j,1} Y_{j,2} \rangle}{\langle Y_{i,1} Y_{i,2} Y_{j,1} Y_{j,2} \rangle}, \end{aligned} \quad (\text{B15})$$

where we used the definition

$$E_{ij}^A = \lambda_{ij}^{\alpha} (\theta_i)_{\alpha}^A W_{i,a}^A + \lambda_{ji}^{\alpha} (\theta_j)_{\alpha}^A W_{j,a}^A. \quad (\text{B16})$$

Each of the R -factors (B14) is completely antisymmetric in the lower indices and of homogeneous degree two in the Grassmann variables $(\theta_i)_{\alpha}^a$. Graphs that can contribute to the loop-integrand $G_4^{(\ell)}$ yield expressions that contain products of exactly 2ℓ R -factors. In order to contribute to the final result, such products must contain the unique product $\theta_5^4 \dots \theta_{4+\ell}^4$ of all non-zero Grassmann variables.

Appendix C: Grassmann contraction

As explained in the main text, we are applying the iterative procedure (16) to numerically perform the Grassmann algebra required to evaluate the twistor expression. The algorithm starts by multiplying the first two

| a | size | N_a |
|-----|-----------------------------------|-----------|
| 1 | $4845 \times 190 \times 190$ | 29 070 |
| 2 | $38760 \times 4845 \times 190$ | 581 400 |
| 3 | $125970 \times 38760 \times 190$ | 3 527 160 |
| 4 | $184756 \times 125970 \times 190$ | 8 314 020 |
| 5 | $125970 \times 184756 \times 190$ | 8 314 020 |
| 6 | $38760 \times 125970 \times 190$ | 3 527 160 |
| 7 | $4845 \times 38760 \times 190$ | 581 400 |
| 8 | $190 \times 4845 \times 190$ | 29 070 |
| 9 | $1 \times 190 \times 190$ | 190 |

TABLE III. Properties of the order-three tensors t_a appearing in the algorithm for the Grassmann contraction (16). Listed are the respective sizes of the tensors, as well as the number of non-zero entries N_a .

R -factors to a purely quartic polynomial with $\binom{20}{4} = 4845$ terms corresponding to all ordered products of four Grassmann variables. Then, this intermediate result is multiplied with the next R -factor, arriving at a polynomial of a degree six. In this manner, we successively multiply one R -factor at a time, eventually arriving at the final unique product involving all 20 Grassmann numbers. At each intermediate step, the degree $2a$ polynomial is represented as a vector of $\binom{20}{2a}$ coefficients, and the multiplication is performed by an order-three tensor t_{a-1} of size $\binom{20}{2a} \times \binom{20}{2a-2} \times \binom{20}{2}$, whose non-zero entries are ± 1 . The number of non-zero elements of each tensor can be computed by

$$N_{a-1} = \binom{2a}{2} \times \binom{20}{2a}. \quad (\text{C1})$$

The first factor counts the number of ways to decompose a degree $2a$ monomial into two monomials of degrees 2 and $2a - 2$, while the second factor corresponds to the number of terms in a degree $2a$ polynomial (i. e. the range of the last index of t_{a-1}). As such, the tensors are very sparse, facilitating the computation. We summarize the properties of the tensors in Table III.

We can estimate the total computation time required to evaluate the integrand numerically on a single kinematic point: We need to add the contributions of ≈ 87 M graphs (see Table II). For each graph, $\sum_{a=1}^9 N_a \approx 25$ M numerical multiplications must be performed, and equally many additions. Assuming 8 FLOPS per cycle per core (using AVX instructions), 3 GHz clock speed and 24 cores, computing one data point would need

$$T \approx \frac{2 \times 87 \times 25 \times 10^{12}}{24 \times 8 \times 3 \times 10^9/\text{s}} \approx 128 \text{ Minutes}. \quad (\text{C2})$$

However, performing the computation with MATHEMATICA on an AMD EPYC 74F3 24-core CPU, we find that the above estimate is significantly over-optimistic, and that the actual runtime is about two orders of magnitude bigger. The most likely reason is that our process is I/O-bound, i. e. the CPU cannot be fed with data fast enough to use its full potential (the tensors do not fit in the L1 cache). Also, MATHEMATICA might not be optimized for this type of operation.

Since the numerical computation is highly parallelizable, we opt to run the sequence of ten sparse tensor-

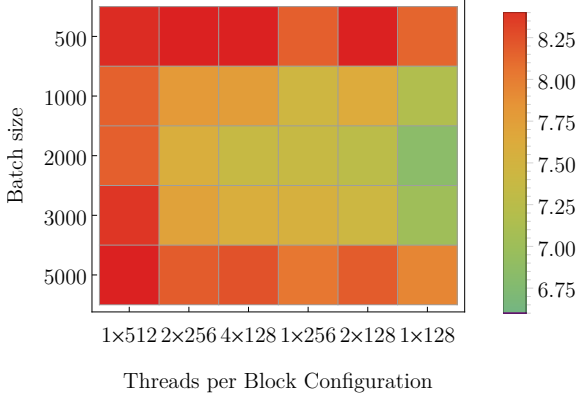


FIG. 3. Heat map showing the time (in seconds) to perform 10,000 five-loop contractions on an *Nvidia A100* GPU. The y-axis represents the batch size, and the x-axis corresponds to the threads-per-block configuration.

vector-vector multiplications on a GPU, which significantly accelerates the computation. We use the `cuda.jit` decorator from the Python package Numba [63], which compiles the function into a custom CUDA kernel for efficient parallel execution. For each $a \in \{2, \dots, 10\}$, the kernel distributes the work of iterating over non-zero entries of the tensor t_{a-1} across CUDA threads, each of which independently multiplies a single non-zero tensor element with the corresponding values in the input vectors S_{a-1} and R_a . The partial product is then atomically accumulated into the output vector S_a to avoid race conditions.

To achieve high performance, we adopt a batched processing strategy in which multiple tensor-vector-vector multiplications of the same tensor but different R -factors are executed simultaneously. This batch dimension allows us to better utilize GPU resources and increase thread occupancy. For each multiplication, the kernel launch configuration uses a specified number of threads per block and blocks per grid, which control the parallel decomposition of the workload. Over all contractions, we use a fixed number of threads per block, while the number of blocks per grid is computed dynamically based on the number of non-zero elements in each tensor and the batch size. The values of the thread block size and batch dimension were tuned through performance benchmarking to maximize throughput on the GPU (see Figure 3). With optimal setting of these parameters, we find that the Grassmann contractions involved when evaluating the twistor expression for one numerical kinematic point takes roughly 17 hours on a single *Nvidia A100* GPU. The code for this procedure can be found in the ancillary file `07-numbaContract5Loop.py` at.

The numerical implementation of this contraction entails a significant precision loss, such that not even `float64` numbers are sufficient to ensure accurate results. For this reason, we opt to evaluate both the twistor expression and the ansatz of the integrand using `int32` integers within a finite field \mathbb{F}_p . To ensure the intermediate values remain within the bounds of the `int32` format,

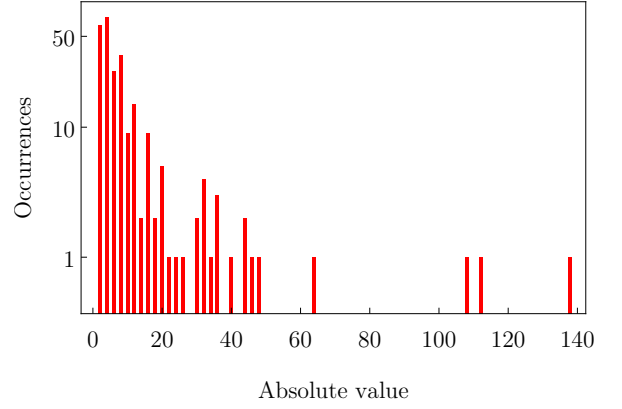


FIG. 4. Histogram of absolute values in the particular genus-one five-loop integrand solution provided in the ancillary files, excluding 582 zero coefficients.

each tensor contraction must produce results that do not exceed the 32 bit integer limit. Considering that the tensor multiplications involve at most 190 summands, we require that $190p^2 < 2^{31}$, which implies that the largest prime we can safely use is given by $p = 3361$.

In the first instance, the particular solution (match between ansatz and twistor expression) will only be valid over the finite field \mathbb{F}_{3361} . However, tuning the result by adding suitable combinations of the 208 Gram identities, we can construct a particular solution where the majority of the 930 f -graph coefficients is zero, and all others attain small integer values (see Figure 4). We expect this to be the true solution over the real numbers. As a check, we compare the particular solution against the twistor expression a few times over different finite fields (\mathbb{F}_{3347} and \mathbb{F}_{3359}). We find perfect agreement, which proves the validity of the solution beyond reasonable doubt.

Appendix D: Non-Planar Master Integrals

In order to compute the sum of integrals (23) that produces the Konishi anomalous dimension, we need to evaluate two non-planar four-loop master integrals that have not been computed before. Explicitly, the unknown integrals read (with $D = 4 - 2\epsilon$)

$$\mathcal{I}_3 = \frac{1}{\pi^4} \int \frac{d^D x_6 d^D x_7 d^D x_8 d^D x_9}{x_{17}^2 x_{18}^2 x_{19}^2 x_{57}^2 x_{58}^2 x_{59}^2 x_{67}^2 x_{68}^2 x_{69}^2}, \quad (\text{D1})$$

$$\mathcal{I}_4 = \frac{1}{\pi^4} \int \frac{d^D x_6 d^D x_7 d^D x_8 d^D x_9}{x_{16}^2 x_{17}^2 x_{18}^2 x_{19}^2 x_{56}^2 x_{57}^2 x_{58}^2 x_{59}^2 x_{67}^2 x_{78}^2 x_{89}^2 x_{69}^2},$$

see Figure 5 for their diagrammatic representation. Expanding the integrals to linear order in ϵ with a priori undetermined coefficients yields (setting $x_{15}^2 = 1$)

$$\mathcal{I}_3 = \frac{a_3}{\epsilon} + b_3 + c_3 \epsilon + \mathcal{O}(\epsilon^2),$$

$$\mathcal{I}_4 = \frac{a_4}{\epsilon} + b_4 + c_4 \epsilon + \mathcal{O}(\epsilon^2). \quad (\text{D2})$$

To constrain the six unknown coefficients, we begin by deriving relations between the 24 master integrals by making use of the Gram identities. As discussed around (7),

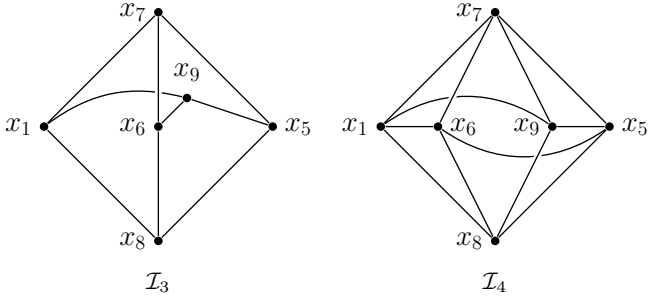


FIG. 5. Diagrammatic representation of the two non-planar four-loop master integrals that contribute to the Konishi anomalous dimension. The edges connecting vertices i and j stand for factors $1/x_{ij}^2$.

these identities manifest as 208 linear relations among the nine-point f -graphs. By following the same steps that led to (23), we can transform these identities to relations among the 24 two-point four-loop master integrals.

First, we normalize the Gram identities among f -graphs in analogy to (19). We then take the OPE limit ($x_2 \rightarrow x_1$, $x_4 \rightarrow x_3$), followed by $x_3 \rightarrow \infty$, and finally integrate over points x_6, \dots, x_9 in $D = 4 - 2\epsilon$ dimensions. Thus, we again arrive at four-loop propagator-type integrals, that can be reduced to a set of master integrals using FIRE6. In fact, they reduce to the same set of 24 master integrals that already appear in the computation of $\gamma_K^{(1,5)}$. Thus the Gram identities turn into linear relations among the 24 master integrals, with ϵ -dependent coefficients.

Plugging in the expressions (ϵ expansions) of the 20 known planar integrals [41, 42] and the two known non-planar ones [38], we find constraints among the coefficients in (D2). The constraints can be brought to the following form:

$$\begin{aligned} a_3 &= 0, \quad b_3 = 36\zeta_3^2, \\ a_4 &= -10\zeta_5, \quad b_4 = -\frac{5\pi^6}{189} + 2\zeta_3^2 + 50\zeta_5, \\ c_4 &= -\frac{32}{27}c_3 + \frac{25\pi^6}{189} + \frac{67}{45}\pi^4\zeta_3 + \frac{226}{3}\zeta_3^2 + 90\zeta_5 - \frac{1143}{2}\zeta_7. \end{aligned} \quad (\text{D3})$$

In total, four of the coefficients are fixed, while the remaining two at linear order in ϵ are related by one equation. Notably, \mathcal{I}_3 is finite in ϵ . Let us mention, that this solution is formulated in the G -scheme used also in [41, 42].

To determine the final two coefficients c_3 and c_4 , we evaluate \mathcal{I}_3 , which is linearly reducible: The integrations can be performed iteratively in a way that each intermediate integral is a hyperlogarithm. In addition, \mathcal{I}_3 involves comparatively few factors $1/x_{ij}^2$, and therefore can be evaluated with HyperInt [64]. We Fourier transform the integral to momentum representation using

$$\mathcal{F}\left[\frac{1}{x^2}\right] = \frac{1}{\pi^{2-\epsilon}} \int d^{4-2\epsilon}x \frac{e^{ipx}}{x^2} = 4^{1-\epsilon} \frac{\Gamma(1-\epsilon)}{(p^2)^{1-\epsilon}}, \quad (\text{D4})$$

and evaluate the momentum integrals with non-integer propagator exponents. In this way, we obtain the ϵ -expansion of \mathcal{I}_3 . The result validates the values of a_3 and b_3 found in (D3), and determines the value of c_3 .

Finally, c_4 is obtained from the last equation in (D3):

$$\begin{aligned} c_3 &= \frac{6\pi^4}{5}\zeta_3 + 72\zeta_3^2 - 567\zeta_7, \\ c_4 &= \frac{25\pi^6}{189} + \frac{\pi^4}{15}\zeta_3 - 10\zeta_3^2 + 90\zeta_5 + \frac{201}{2}\zeta_7. \end{aligned} \quad (\text{D5})$$

We verify the solution of the integrals \mathcal{I}_3 and \mathcal{I}_4 numerically using FIESTA [65] up to four digits in precision, and find perfect agreement with our exact coefficients.

-
- [1] F. Gonzalez-Rey, I. Y. Park, and K. Schalm, A note on four point functions of conformal operators in $\mathcal{N} = 4$ superYang–Mills, *Phys. Lett. B* **448**, 37 (1999), [arXiv:hep-th/9811155](#).
 - [2] B. Eden, P. S. Howe, C. Schubert, E. Sokatchev, and P. C. West, Four point functions in $\mathcal{N} = 4$ supersymmetric Yang–Mills theory at two loops, *Nucl. Phys. B* **557**, 355 (1999), [arXiv:hep-th/9811172](#).
 - [3] B. Eden, P. S. Howe, C. Schubert, E. Sokatchev, and P. C. West, Simplifications of four point functions in $\mathcal{N} = 4$ supersymmetric Yang–Mills theory at two loops, *Phys. Lett. B* **466**, 20 (1999), [arXiv:hep-th/9906051](#).
 - [4] B. Eden, C. Schubert, and E. Sokatchev, Three loop four point correlator in $\mathcal{N} = 4$ SYM, *Phys. Lett. B* **482**, 309 (2000), [arXiv:hep-th/0003096](#).
 - [5] M. Bianchi, S. Kovacs, G. Rossi, and Y. S. Stanev, Anomalous dimensions in $\mathcal{N} = 4$ SYM theory at order g^{*4} , *Nucl. Phys. B* **584**, 216 (2000), [arXiv:hep-th/0003203](#).
 - [6] B. Eden, P. Heslop, G. P. Korchemsky, and E. Sokatchev, Hidden symmetry of four-point correlation functions and amplitudes in $\mathcal{N} = 4$ SYM, *Nucl. Phys. B* **862**, 193 (2012), [arXiv:1108.3557 \[hep-th\]](#).
 - [7] B. Eden, P. Heslop, G. P. Korchemsky, and E. Sokatchev, Constructing the correlation function of four stress-tensor multiplets and the four-particle amplitude in $\mathcal{N} = 4$ SYM, *Nucl. Phys. B* **862**, 450 (2012), [arXiv:1201.5329 \[hep-th\]](#).
 - [8] R. G. Ambrosio, B. Eden, T. Goddard, P. Heslop, and C. Taylor, Local integrands for the five-point amplitude in planar $\mathcal{N} = 4$ SYM up to five loops, *JHEP* **01**, 116, [arXiv:1312.1163 \[hep-th\]](#).
 - [9] J. L. Bourjaily, P. Heslop, and V.-V. Tran, Perturbation theory at eight loops: Novel structures and the breakdown of manifest conformality in $\mathcal{N} = 4$ supersymmetric Yang–Mills theory, *Phys. Rev. Lett.* **116**, 191602 (2016), [arXiv:1512.07912 \[hep-th\]](#).
 - [10] J. L. Bourjaily, P. Heslop, and V.-V. Tran, Amplitudes and correlators to ten loops using simple, graphical bootstraps, *JHEP* **11**, 125, [arXiv:1609.00007 \[hep-th\]](#).
 - [11] S. He, C. Shi, Y. Tang, and Y.-Q. Zhang, The cusp limit of correlators and a new graphical bootstrap for correlators/amplitudes to eleven loops, *JHEP* **03**, 192, [arXiv:2410.09859 \[hep-th\]](#).
 - [12] J. L. Bourjaily, S. He, C. Shi, and Y. Tang, The four-point correlator of planar sym at twelve loops, (2025), [arXiv:2503.15593 \[hep-th\]](#).
 - [13] E. D’Hoker, D. Z. Freedman, S. D. Mathur, A. Matusis, and L. Rastelli, Graviton exchange and complete four point functions in the AdS/CFT correspondence, *Nucl. Phys. B* **562**, 353 (1999), [arXiv:hep-th/9903196 \[hep-th\]](#).
 - [14] E. D’Hoker, D. Z. Freedman, and L. Rastelli, AdS/CFT four point functions: How to succeed at z integrals without really trying, *Nucl. Phys. B* **562**, 395 (1999), [arXiv:hep-th/9905049 \[hep-th\]](#).
 - [15] G. Arutyunov and S. Frolov, Four point functions of lowest weight cpos in $\mathcal{N} = 4$ SYM(4) in supergravity ap-

- proximation, *Phys. Rev. D* **62**, 064016 (2000), [arXiv:hep-th/0002170](#).
- [16] L. Rastelli and X. Zhou, Mellin amplitudes for supergravity on $AdS_5 \times S^5$, *Phys. Rev. Lett.* **118**, 091602 (2017), [arXiv:1608.06624 \[hep-th\]](#).
- [17] L. F. Alday and A. Bissi, Loop corrections to supergravity on $AdS_5 \times S^5$, *Phys. Rev. Lett.* **119**, 171601 (2017), [arXiv:1706.02388 \[hep-th\]](#).
- [18] F. Aprile, J. M. Drummond, P. Heslop, and H. Paul, Quantum gravity from conformal field theory, *JHEP* **01**, 035, [arXiv:1706.02822 \[hep-th\]](#).
- [19] L. Rastelli and X. Zhou, How to succeed at holographic correlators without really trying, *JHEP* **04**, 014, [arXiv:1710.05923 \[hep-th\]](#).
- [20] E. Y. Yuan, Simplicity in AdS perturbative dynamics, (2018), [arXiv:1801.07283 \[hep-th\]](#).
- [21] D. Carmi, Loops in AdS: From the spectral representation to position space, *JHEP* **06**, 049, [arXiv:1910.14340 \[hep-th\]](#).
- [22] J. M. Drummond and H. Paul, One-loop string corrections to AdS amplitudes from CFT, *JHEP* **03**, 038, [arXiv:1912.07632 \[hep-th\]](#).
- [23] Z. Huang and E. Y. Yuan, Graviton scattering in $AdS_5 \times S^5$ at two loops, *JHEP* **04**, 064, [arXiv:2112.15174 \[hep-th\]](#).
- [24] J. M. Drummond and H. Paul, Two-loop supergravity on $AdS_5 \times S^5$ from CFT, *JHEP* **08**, 275, [arXiv:2204.01829 \[hep-th\]](#).
- [25] S. Caron-Huot, F. Coronado, A.-K. Trinh, and Z. Zahraee, Bootstrapping $\mathcal{N} = 4$ sym correlators using integrability, *JHEP* **02**, 083, [arXiv:2207.01615 \[hep-th\]](#).
- [26] Z. Huang, B. Wang, and E. Y. Yuan, A differential representation for holographic correlators, *JHEP* **07**, 176, [arXiv:2403.10607 \[hep-th\]](#).
- [27] S. Caron-Huot, F. Coronado, and Z. Zahraee, Bootstrapping $\mathcal{N} = 4$ sym correlators using integrability and localization, *JHEP* **05**, 220, [arXiv:2412.00249 \[hep-th\]](#).
- [28] A. V. Belitsky, S. Hohenegger, G. P. Korchemsky, E. Sokatchev, and A. Zhiboedov, From correlation functions to event shapes, *Nucl. Phys. B* **884**, 305 (2014), [arXiv:1309.0769 \[hep-th\]](#).
- [29] A. V. Belitsky, S. Hohenegger, G. P. Korchemsky, E. Sokatchev, and A. Zhiboedov, Event shapes in $\mathcal{N} = 4$ super-Yang-Mills theory, *Nucl. Phys. B* **884**, 206 (2014), [arXiv:1309.1424 \[hep-th\]](#).
- [30] A. V. Belitsky, S. Hohenegger, G. P. Korchemsky, E. Sokatchev, and A. Zhiboedov, Energy-energy correlations in $\mathcal{N} = 4$ supersymmetric Yang-Mills theory, *Phys. Rev. Lett.* **112**, 071601 (2014), [arXiv:1311.6800 \[hep-th\]](#).
- [31] K. A. Intriligator, Bonus symmetries of $\mathcal{N} = 4$ super-Yang-Mills correlation functions via AdS duality, *Nucl. Phys. B* **551**, 575 (1999), [arXiv:hep-th/9811047 \[hep-th\]](#).
- [32] B. Eden, P. S. Howe, C. Schubert, E. Sokatchev, and P. C. West, Extremal correlators in four-dimensional SCFT, *Phys. Lett. B* **472**, 323 (2000), [arXiv:hep-th/9910150 \[hep-th\]](#).
- [33] T. Fleury and R. Pereira, Non-planar data of $\mathcal{N} = 4$ SYM, *JHEP* **03**, 003, [arXiv:1910.09428 \[hep-th\]](#).
- [34] B. Eden, A. C. Petkou, C. Schubert, and E. Sokatchev, Partial non-renormalisation of the stress-tensor four-point function in $\mathcal{N} = 4$ SYM₄ and AdS/CFT, *Nucl. Phys. B* **607**, 191 (2001), [hep-th/0009106](#).
- [35] G. Brinkmann, A practical algorithm for the computation of the genus, *Ars Mathematica Contemporanea* **22** (2022).
- [36] L. F. Alday, B. Eden, G. P. Korchemsky, J. Maldacena, and E. Sokatchev, From correlation functions to Wilson loops, *JHEP* **1109**, 123, [arXiv:1007.3243 \[hep-th\]](#).
- [37] The Sage Developers, *SageMath, the Sage Mathematics Software System (Version 10.7)* (2025).
- [38] B. Eden, P. Heslop, G. P. Korchemsky, V. A. Smirnov, and E. Sokatchev, Five-loop Konishi in $\mathcal{N} = 4$ SYM, *Nucl. Phys. B* **862**, 123 (2012), [arXiv:1202.5733 \[hep-th\]](#).
- [39] A. V. Smirnov and F. S. Chukharev, FIRE6: Feynman Integral REduction with modular arithmetic, *Comput. Phys. Commun.* **247**, 106877 (2020), [arXiv:1901.07808 \[hep-ph\]](#).
- [40] A. V. Smirnov and M. Zeng, FIRE 6.5: Feynman integral reduction with new simplification library, *Comput. Phys. Commun.* **302**, 109261 (2024), [arXiv:2311.02370 \[hep-ph\]](#).
- [41] P. A. Baikov and K. G. Chetyrkin, Four loop massless propagators: An algebraic evaluation of all master integrals, *Nucl. Phys. B* **837**, 186 (2010), [arXiv:1004.1153 \[hep-ph\]](#).
- [42] R. N. Lee, A. V. Smirnov, and V. A. Smirnov, Master integrals for four-loop massless propagators up to transcendentality weight twelve, *Nucl. Phys. B* **856**, 95 (2012), [arXiv:1108.0732 \[hep-th\]](#).
- [43] D. J. Broadhurst and D. Kreimer, Knots and numbers in ϕ^4 theory to 7 loops and beyond, *Int. J. Mod. Phys. C* **6**, 519 (1995), [arXiv:hep-ph/9504352](#).
- [44] F. Brown and O. Schnetz, Proof of the zig-zag conjecture, (2012), [arXiv:1208.1890 \[math.NT\]](#).
- [45] S. Leurent and D. Volin, Multiple zeta functions and double wrapping in planar $\mathcal{N} = 4$ SYM, *Nucl. Phys. B* **875**, 757 (2013), [arXiv:1302.1135 \[hep-th\]](#).
- [46] V. N. Velizhanin, The non-planar contribution to the four-loop universal anomalous dimension in $\mathcal{N} = 4$ supersymmetric Yang-Mills theory, *JETP Lett.* **89**, 593 (2009), [arXiv:0902.4646 \[hep-th\]](#).
- [47] S.-Q. Zhang, Nonplanar integrated correlator in $\mathcal{N} = 4$ SYM, *Phys. Rev. D* **110**, 025003 (2024), [arXiv:2404.18900 \[hep-th\]](#).
- [48] D. Dorigoni, M. B. Green, and C. Wen, Novel representation of an integrated correlator in $\mathcal{N} = 4$ supersymmetric Yang-Mills theory, *Phys. Rev. Lett.* **126**, 161601 (2021), [arXiv:2102.08305 \[hep-th\]](#).
- [49] D. Dorigoni, M. B. Green, and C. Wen, Exact properties of an integrated correlator in $\mathcal{N} = 4$ su(n) SYM, *JHEP* **05**, 089, [arXiv:2102.09537 \[hep-th\]](#).
- [50] A. Georgoudis, V. Gonçalves, and R. Pereira, Konishi ope coefficient at the five loop order, *JHEP* **11**, 184, [arXiv:1710.06419 \[hep-th\]](#).
- [51] J. M. Henn, G. P. Korchemsky, and B. Mistlberger, The full four-loop cusp anomalous dimension in $\mathcal{N} = 4$ super Yang-Mills and QCD, *JHEP* **04**, 018, [arXiv:1911.10174 \[hep-th\]](#).
- [52] D. Anselmi, M. T. Grisaru, and A. Johansen, A critical behavior of anomalous currents, electric - magnetic universality and CFT in four-dimensions, *Nucl. Phys. B* **491**, 221 (1997), [arXiv:hep-th/9601023](#).
- [53] A. V. Kotikov, L. N. Lipatov, A. I. Onishchenko, and V. N. Velizhanin, Three-loop universal anomalous dimension of the Wilson operators in $\mathcal{N} = 4$ SUSY Yang-Mills model, *Phys. Lett. B* **595**, 521 (2004), [hep-th/0404092](#).
- [54] F. Fiamberti, A. Santambrogio, C. Sieg, and D. Zanon, Anomalous dimension with wrapping at four loops in $\mathcal{N} = 4$ SYM, *Nucl. Phys. B* **805**, 231 (2008), [arXiv:0806.2095 \[hep-th\]](#).
- [55] V. N. Velizhanin, The four-loop anomalous dimension of the Konishi operator in $\mathcal{N} = 4$ supersymmetric Yang-Mills theory, *JETP Lett.* **89**, 6 (2009), [arXiv:0808.3832 \[hep-th\]](#).
- [56] Z. Bajnok and R. A. Janik, Four-loop perturbative konishi from strings and finite size effects for multiparticle states, *Nucl. Phys. B* **807**, 625 (2009), [arXiv:0807.0399 \[hep-th\]](#).

- [57] Z. Bajnok, A. Hegedus, R. A. Janik, and T. Lukowski, Five loop Konishi from AdS/CFT, *Nucl. Phys. B* **827**, 426 (2010), [arXiv:0906.4062 \[hep-th\]](#).
- [58] G. Arutyunov, S. Frolov, and R. Suzuki, Five-loop konishi from the mirror TBA, *JHEP* **04**, 069, [arXiv:1002.1711 \[hep-th\]](#).
- [59] J. Balog and A. Hegedus, 5-loop Konishi from linearized TBA and the xxx magnet, *JHEP* **06**, 080, [arXiv:1002.4142 \[hep-th\]](#).
- [60] N. Beisert, B. Eden, and M. Staudacher, Transcendentality and crossing, *J. Stat. Mech.* **07**, P01021 (2007), [hep-th/0610251](#).
- [61] R. Boels, L. J. Mason, and D. Skinner, Supersymmetric gauge theories in twistor space, *JHEP* **02**, 014, [arXiv:hep-th/0604040](#).
- [62] D. Chicherin, R. Doobary, B. Eden, P. Heslop, G. P. Korchemsky, L. Mason, and E. Sokatchev, Correlation functions of the chiral stress-tensor multiplet in $\mathcal{N} = 4$ SYM, *JHEP* **06**, 198, [arXiv:1412.8718 \[hep-th\]](#).
- [63] S. K. Lam, A. Pitrou, and S. Seibert, Numba: a LLVM-based python JIT compiler, in *Proceedings of the Second Workshop on the LLVM Compiler Infrastructure in HPC*, LLVM '15 (Association for Computing Machinery, New York, NY, USA, 2015).
- [64] E. Panzer, Algorithms for the symbolic integration of hyperlogarithms with applications to Feynman integrals, *Comput. Phys. Commun.* **188**, 148 (2015), [arXiv:1403.3385 \[hep-th\]](#).
- [65] A. V. Smirnov, N. D. Shapurov, and L. I. Vysotsky, FI-ESTA5: Numerical high-performance Feynman integral evaluation, *Comput. Phys. Commun.* **277**, 108386 (2022), [arXiv:2110.11660 \[hep-ph\]](#).